Central limit behavior at the edge of chaos in the z-logistic map

Abbas Ali Saberi [1,2,3,*] Ugur Tirnakli [4,5,†] and Constantino Tsallis [6,7,8,‡]

[1]*School of Science, Constructor University, Campus Ring 1, 28759 Bremen, Germany*
[2]*Max Planck Institute for the Physics of Complex Systems, 01187 Dresden, Germany*
[3]*Department of Physics, University of Tehran, P. O. Box 14395-547, Tehran, Iran*
[4]*Department of Physics, Faculty of Arts and Sciences, Izmir University of Economics, 35330 Izmir, Turkey*
[5]*Complex Systems Research and Application Center, Izmir University of Economics, 35330 Izmir, Turkey*
[6]*Centro Brasileiro de Pesquisas Fisicas and National Institute of Science and Technology of Complex Systems, Rua Xavier Sigaud 150, Rio de Janeiro, Brazil*
[7]*Santa Fe Institute, 1399 Hyde Park Road, New Mexico 87501, USA*
[8]*Complexity Science Hub Vienna, Metternichgasse 8, 1030 Vienna, Austria*

(Received 6 August 2025; accepted 12 November 2025; published 9 December 2025)

We focus on the Feigenbaum-Coullet-Tresser point of the dissipative one-dimensional z-logistic map $x_{t+1} = 1 - a|x_t|^z$ ($z \geqslant 1$). We show that sums of iterates converge to q-Gaussian distributions $P_q(y) = P_q(0)\exp_q(-\beta_q y^2) = P_q(0)[1 + (q-1)\beta_q y^2]^{1/(1-q)}$ ($q \geqslant 1; \beta_q > 0$), which optimize the nonadditive entropic functional S_q under simple constraints. We propose and justify heuristically a closed-form prediction for the entropic index, $q(z) = 1 + 2/(z+1)$, and validate it numerically via data collapse for typical z values. The formula captures how the limiting law depends on the nonlinearity order and implies finite variance for $z > 2$ and divergent variance for $1 \leqslant z \leqslant 2$. These results extend edge-of-chaos central limit behavior beyond the standard ($z = 2$) case and provide a simple predictive law for unimodal maps with varying maximum order.

DOI: 10.1103/gtlz-67cf

I. INTRODUCTION

In the study of dynamical systems theory, one of the most important and widely used workhorses is, no doubt, the logistic map. For discrete cases, it is a fundamental model commonly used to study population dynamics, chaos, and bifurcation phenomena. Mathematicians mostly like to use the definition given as

$$X_{t+1} = r\,X_t(1 - X_t), \tag{1}$$

where $0 \leqslant r \leqslant 4$ is a parameter that governs the behavior of the map (frequently called the control parameter), and $X_t \in [0, 1]$ is the state variable at iteration $t = 0, 1, 2, \ldots$ [1,2]. It has long been known that the logistic map exhibits a variety of dynamical behavior, ranging from fixed points to chaotic regimes with periodic windows as the parameter r is varied. On the other hand, most physicists prefer to use the definition in the form

$$x_{t+1} = 1 - a|x_t|^2, \tag{2}$$

where $0 \leqslant a \leqslant 2$ and $x_t \in [-1, 1]$ are the new map parameter and the state variable, respectively. It is easy to show that the definitions (1) and (2) are topologically conjugated and can be transformed into each other using a conjugation function [3]. Various types of generalizations for the standard logistic map can be found in the literature [4–11]. Here, we study the generalized version based on the definition in Eq. (2), introducing an additional parameter z which allows us to control the degree of nonlinearity of the system at its maximal point. Therefore, the *generalized z-logistic map* is defined as follows,

$$x_{t+1} = 1 - a|x_t|^z, \quad 0 \leqslant a \leqslant 2, \tag{3}$$

where $z \geqslant 1$ controls the power to which the state variable $x_t \in [-1, 1]$ is raised, introducing a wider range of topologically isomorphic dynamic behaviors, though metrically different from the classical logistic map, as can be seen from Fig. 1(a). As z increases, the map becomes more chaotic in the sense that fixing a in the chaotic regime (e.g., $a = 2$) and increasing z strengthen the chaos metrically [12]. The parameter a governs the overall structure of the map. Similarly to the standard logistic map ($z = 2$), varying a triggers transitions of the system from stable fixed points to periodic orbits and eventually chaotic behavior as depicted in Fig. 1(b). From this figure and from an earlier work [13], one can also easily see that the chaos threshold point $a_c(z)$ (defined as the critical point where the system enters into the chaotic region via period doublings of successive bifurcations) tends to 1 as $z \to 1$, while it comes closer to 2 as $z \to \infty$, suppressing the chaotic region of the map. Some values of a_c are given in Table I for representative values of z.

*Contact author: asaberi@constructor.university
†Contact author: ugur.tirnakli@ieu.edu.tr
‡Contact author: tsallis@cbpf.br

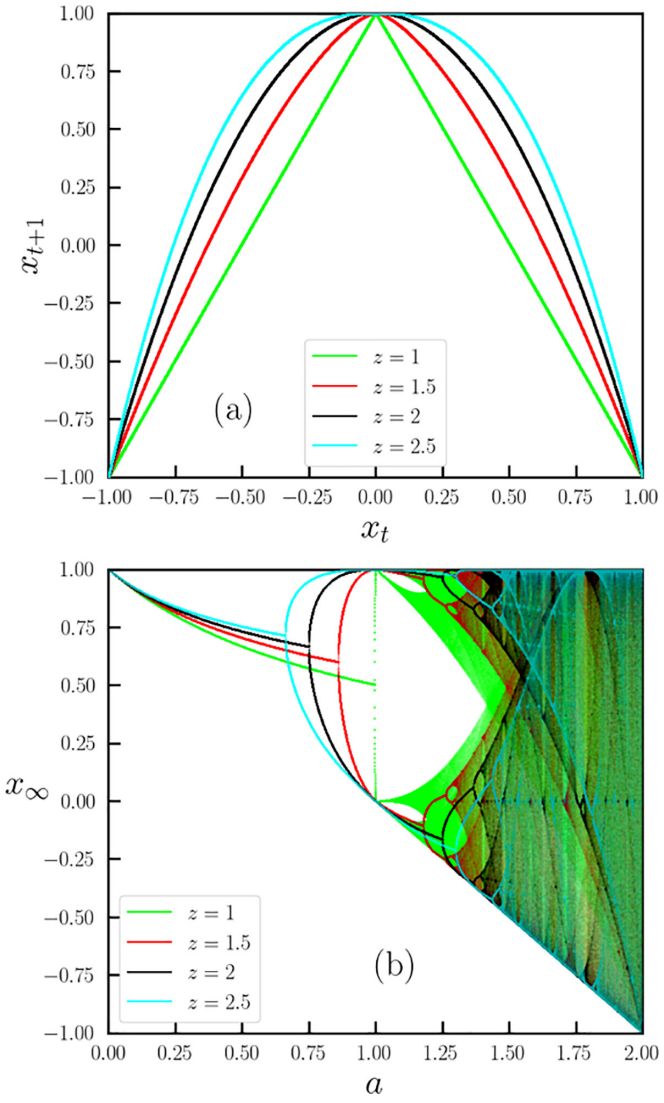

FIG. 1. (a) Phase portrait and (b) bifurcation diagram of the z-logistic map for some representative values of z.

We provide a closed-form prediction for the nonadditive index that governs the central limit attractor of sums of iterates of the z-logistic map at the Feigenbaum-Coullet-Tresser point. Specifically, we predict

$$q(z) = 1 + \frac{2}{z+1} \quad (z \geqslant 1). \tag{4}$$

TABLE I. a_c, q, $\bar{\beta}_q$, and $\delta_F(z)$ values for various z of the z-logistic map.

z	a_c	q	$\bar{\beta}_q$	$\delta_F(z)$
1	1	2	π^2	
1.75	1.35506075662336 …	1.727 …	6.489 …	4.2571 …
1.85	1.37474875895489 …	1.702 …	6.278 …	4.4261 …
2	1.40115518909205 …	1.667 …	6.002 …	4.6992 …
2.15	1.42456107409069 …	1.635 …	5.768 …	4.9017 …
2.25	1.43880058172258 …	1.615 …	5.630 …	5.0518 …
∞	2	1	π	

This relation is obtained from a tail-moment argument tied to the order z of the map's maximum. The index is not fitted; accordingly, the limiting q-Gaussian has a fixed shape (no free shape parameter), and only an overall scale is estimated from data. Using Huberman-Rudnick scaling to coordinate the approach to criticality with the number of summands, we validate this prediction across several z values by data collapse of rescaled sums onto the corresponding q-Gaussians. Importantly, the $q(z)$ introduced here characterizes the statistics of sum distributions at the edge of chaos and should not be confused with indices such as q_{sen} that quantify sensitivity to initial conditions; such indices need not to coincide in this setting.

II. CENTRAL LIMIT BEHAVIOR

Now we are in a position to discuss the Central Limit (CL) behavior of this system. As is well known, the classical CL theorem applies to sums of independent and identically distributed (i.i.d.) random variables. In any kind of real or model systems with such random variables, as the number of variables increases, the distribution of their sum converges to a Gaussian distribution. More precisely, one can write

$$y = \frac{1}{\sqrt{T}} \sum_{i=1}^{T} (x_i - \langle x \rangle), \tag{5}$$

where T is the number of summands, x is the random variable of the system considered, and $\langle \cdots \rangle$ defines an average over a large number T of iterations and a large number of randomly chosen initial values x_1, which can be numerically calculated as

$$\langle x \rangle = \frac{1}{n_{\text{ini}}} \frac{1}{T} \sum_{j=1}^{n_{\text{ini}}} \sum_{i=1}^{T} x_i^{(j)}. \tag{6}$$

In our simulations, we discard the first $T_{\text{trans}} = 2^{15}$ iterates as transients and average over n_{ini} uniformly sampled initial conditions in $[-1, 1]$; results are robust to alternative choices (e.g., deterministic grids). In the case of the z-logistic map, any chaotic point in the phase space, for example, for the $(z = 2, a = 2)$ case, although the iterates of a deterministic map cannot be completely independent, for our random variable y one can still verify the standard CL theorem if the assumption of i.i.d. random variables is replaced by the property that our system is strongly mixing. Therefore, one should expect to have a Gaussian probability distribution as $T \to \infty$, namely

$$P(y) = \frac{1}{\sqrt{2\pi\sigma^2}} \exp\left(-\frac{y^2}{2\sigma^2}\right). \tag{7}$$

This has already been studied in Ref. [14], and Gaussian behavior is observed. In fact, this behavior has also been achieved for other parameter values in the chaotic region. One can argue that the standard CL theorem will be valid if the Lyapunov exponent is positive. On the other hand, when we concentrate on the chaos threshold point where the standard Lyapunov exponent vanishes, the map is not sufficiently strongly mixing and, due to ergodicity breaking, the standard CL theorem is no longer valid. In order to study the CL behavior of such systems, the standard CL theorem has recently been generalized [15–19]. Consistent with generalized

central limit behavior for strongly correlated dynamics, the following q-Gaussian attractors are expected and/or observed under appropriate scaling,

$$P_q(y) = \frac{\sqrt{\beta_q}}{C_q} \exp_q\left(-\beta_q y^2\right), \tag{8}$$

where β_q is a parameter that characterizes the width of the distribution and here $\exp_q(u)$ is known as the q-exponential of the form $[1+(1-q)u]^{\frac{1}{1-q}}$ $(q \geqslant 1)$. As $q \to 1$, this generalized exponential form takes the form of the standard one, hence the Gaussian distribution is recovered. Moreover, all convergence statements for the distributions are understood in the limit $T \to \infty$; at the Feigenbaum point this limit is taken jointly with $|a - a_c(z)| \to 0$ according to the Huberman-Rudnick scaling (Sec. III). The normalization factor C_q can be calculated from Refs. [20,21] and is given by

$$C_q = \begin{cases} \sqrt{\pi}, & q = 1, \\ \frac{\Gamma\left(\frac{3-q}{2q-2}\right)}{\Gamma\left(\frac{1}{q-1}\right)} \sqrt{\frac{\pi}{q-1}}, & 1 < q < 3. \end{cases} \tag{9}$$

Let us remind at this point that distributions (8) optimize, under simple constraints, the nonadditive entropic functional [22]

$$S_q[P(y)] = \frac{1 - \int dy\,[P(y)]^q}{q-1} \quad (q \in \mathbb{R}), \tag{10}$$

which, in the $q \to 1$ limit, recovers the classical Boltzmann-Gibbs (additive) functional

$$S_1[P(y)] = S_{\mathrm{BG}}[P(y)] \equiv -\int dy P(y) \ln P(y). \tag{11}$$

The optimization of these entropic functionals under appropriate constraints yields the probability distributions corresponding to the stationary states. Let us also remind at this point that the infinite-temperature limit within the canonical ensemble corresponds to the microcanonical ensemble.

If the prefactor in front of the q-exponential in Eq. (8) is defined as $P_q(0)$, then one can easily write

$$[yP_q(0)]^2 = \frac{\beta_q}{C_q^2} y^2 \Rightarrow \beta_q y^2 = C_q^2 y^2 [P_q(0)]^2, \tag{12}$$

and, comparing to Eq. (8), we have

$$\frac{P_q(y)}{P_q(0)} = \{1 - (1-q)\bar{\beta}_q [yP_q(0)]^2\}^{\frac{1}{1-q}}, \tag{13}$$

where

$$\bar{\beta}_q = C_q^2. \tag{14}$$

The subtle difficulty in analyzing the system at the edge of chaos (i.e., at $a = a_c$) is that taking $T \to \infty$ alone is not sufficient for the system to achieve its limit distribution. The other ingredient must be to localize the critical point a_c with infinite precision. More precisely, for a full description of the shape of the distribution function on the attractor, a simultaneous limit is needed, as the precision of the a_c value and the number of iterates tend to infinity. However, in numerical experiments, neither the precision of a_c nor the values of T can reach infinity. Therefore, numerically, one needs to focus on the situation as a kind of interplay between the precision of a_c and the number of iterates. In Ref. [23], it has been shown that a successful interplay can be achieved using the Huberman-Rudnick scaling law [24]. Basically, the idea is to find (a, T) tuples from

$$2^{-n} = |a - a_c(z)|^{\ln 2 / \ln \delta_F(z)}, \tag{15}$$

where $\delta_F(z)$ is the z-generalized Feigenbaum constant (calculated numerical values are in Table I) and $n = 1, 2, \ldots, \infty$ which will be used to find the value T to be used ($T = 2^{2n}$) for a particular value of a in the vicinity of $a_c(z)$ (see Ref. [23] for more details). All (a, T) tuples used in this work are given in Table II. Here, we set all values of the parameter a so that the precision of the corresponding $2n$ value would be of the order of 0.05. The CL behavior of the standard logistic map ($z = 2$) has already been numerically analyzed in this way in Refs. [23,25] and the value of q is found to be close to 1.65.

TABLE II. Parameter values used in this work. The values of (a, T) tuples are obtained from the scaling Eq. (15).

z	a	$2n$	$T = 2^{2n}$
1.75	1.3550696971	16.05	2^{16}
	1.3550628567	18.05	2^{18}
	1.3550612499	20.05	2^{20}
1.85	1.3747552996	16.05	2^{16}
	1.3747502366	18.05	2^{18}
	1.3747490928	20.05	2^{20}
2	1.4011592349	16.05	2^{16}
	1.4011560500	18.05	2^{18}
	1.4011553723	20.05	2^{20}
2.15	1.4245639575	16.05	2^{16}
	1.4245616623	18.05	2^{18}
	1.4245611940	20.05	2^{20}
2.25	1.4388028452	16.05	2^{16}
	1.4388010297	18.05	2^{18}
	1.4388006704	20.05	2^{20}

III. RELATION BETWEEN q AND z

In order to relate q and z values of the z-logistic map in Eq. (3), let us assume that the moment $\langle |x|^z \rangle$ of a q-Gaussian is proportional to $\int_0^\infty dx |x|^z \exp_q(-x^2)$, which diverges (logarithmically) for

$$\frac{2}{q-1} - z = 1 \quad (z \geqslant 1). \tag{16}$$

From this condition, we obtain $q = 5/3 = 1.666\ldots$ for $z = 2$. This value obtained from the scaling relation is in fact very close numerically to what has been found earlier in Refs. [23,25] for the standard logistic map. Moreover, the case $z = 1$ (a piecewise-linear unimodal map) yields $q = 2$ from our prediction; this is consistent with increasingly heavy tails at lower z and it has already been known analytically in the literature [26] that this is the genuine distribution for this case (see also Refs. [27–29], where strong chaos emerges discontinuously). These analytic results are not derived at the Feigenbaum point itself; we refer to them to support the expected tail behavior as $z \to 1$, consistent with our heuris-

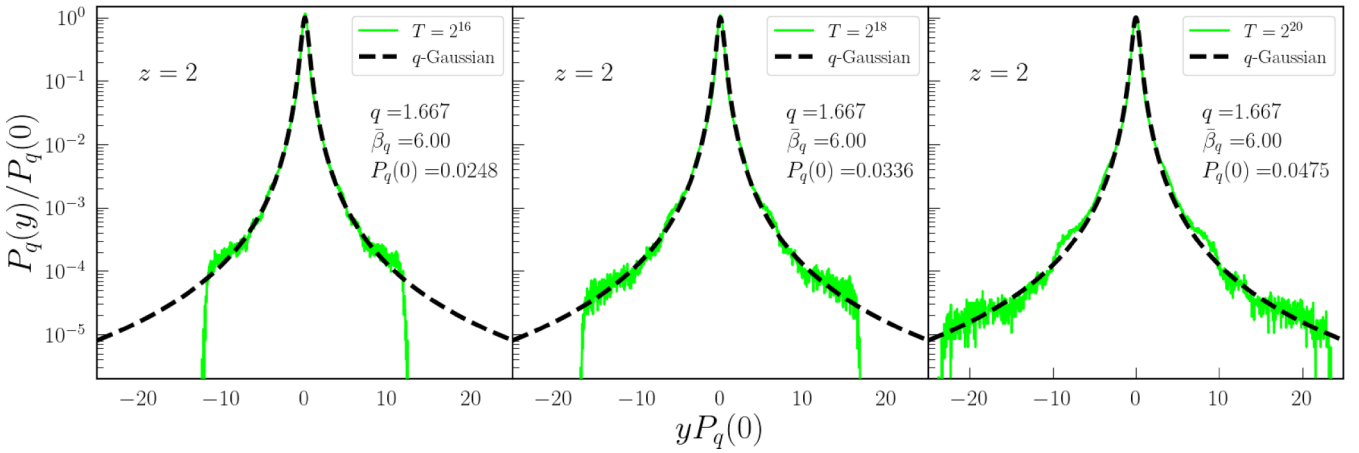

FIG. 2. Normalized probability distribution given by Eq. (13) with increasing T for $z = 2$. For the histogram, we always use 1000 boxes to have equally sized bins for the entire time series from minimum to maximum y values. Notice that here the only fitting parameter for the q-Gaussian (black dashed line) is $P_q(0)$.

tic relation in Eq. (4). Therefore, we have the second point corroborating the scaling given in Eq. (16). It might well be that this scaling applies to *all values of* z. Therefore, the CL behavior of the probability distribution at the z-generalized Feigenbaum-Coullet-Tresser point would be expected to approach a q-Gaussian with the index q *a priori* known from the equation given as indicated in Eq. (4). Consequently, q monotonically decreases from 2 to 1 when z increases from 1 to infinity (notice that, at the $z \to \infty$ limit, the map becomes totally flat, thus approaching the behavior of a random number generator). Notice that the analytically extended $z = 0$ limit implies $q = 3$ (upper bound for normalizability of q-Gaussians). In what follows, we provide numerical support to this conjecture. In the generalized CL theorem framework [15,16], sums of variables whose effective variance diverges converge, after appropriate rescaling, to the q-Gaussian in Eq. (13). For $q > 1$, q-Gaussian has a power-law tail. Setting $u = (q-1)\beta_q y^2 \gg 1$ in Eq. (8) yields

$$P_q(y) \sim u^{1/(1-q)} \sim y^{-\frac{2}{q-1}}. \tag{17}$$

Thus, the asymptotic exponent is $2/(q-1)$. The absolute mth moment is

$$\langle |y|^m \rangle \sim 2\int_{Y_0}^{\infty} y^m\, y^{-\frac{2}{q-1}}\, dy = 2\int_{Y_0}^{\infty} y^{m-\frac{2}{q-1}}\, dy. \tag{18}$$

Convergence at the upper limit requires

$$m - \frac{2}{q-1} < -1, \tag{19}$$

while the threshold of (logarithmic) divergence is

$$m - \frac{2}{q-1} = -1 \Longrightarrow q - 1 = \frac{2}{m+1}. \tag{20}$$

In the standard CL theorem, for i.i.d. linear variables, one takes $m = 2$ (the variance). For the map (3), however, the iteration involves $|x|^z$, so the *natural* moment whose divergence governs the attractor class is the zth moment: $m \longrightarrow z$. Imposing Eq. (20) with $m = z$ directly yields Eq. (4). Clearly, if we refer to the form of Eq. (1), x must be replaced by $(X - 1/2)$. In addition, within the unimodal Feigenbaum universality class, smooth conjugacies preserve the local flatness (critical) order z at the maximum; therefore identifying the divergence threshold with $m = z$—and hence Eq. (4)—is invariant under such conjugacies.

The final step before trying to corroborate the proposed scaling relation with numerical experiments remains to determine the $\bar{\beta}_q$ values from Eq. (14). Some representative values of $(q, \bar{\beta}_q)$ are given in Table I.

IV. NUMERICAL VALIDATION OF $q(z)$

Now we are ready to present our numerical results in order to validate our scaling relation (4) and the corresponding $\bar{\beta}_q$ value from Eq. (14). It is worth noting here that, for a particular z value, q and $\bar{\beta}_q$ are not fitting parameters; they are known *a priori* when we start simulations. Therefore, the only fitting parameter in these simulations is $P_q(0)$. In order to numerically approach this value, let us start from Eq. (13) and assume that $(q-1)\bar{\beta}_q P_q(0)^2 y^2 \gg 1$, which allows us to write

$$P_q(0) = (q-1)^{1/(q-3)} \bar{\beta}_q^{1/(q-3)} \lim_{y\to\infty} P_q(y)^{(q-1)/(q-3)} y^{2/(q-3)}. \tag{21}$$

In the numerics, for a better estimate, we take an average over the values obtained for large y values before the sharp drop is attained.

Another mathematically equivalent path would be to consider β_q, instead of $P_q(0)$, as a fitting parameter. We have used the present path taking advantage of the fact that $\bar{\beta}_q$ is analytically available.

Naturally, as a first case, we reconsider the standard logistic map ($z = 2$). It is evident from Fig. 2 that, as the values of T increase (and the related value a given in Table II is used), the probability distribution develops in the tails of the q-Gaussian whose $(q, \bar{\beta}_q)$ pair comes *a priori* directly from our Eqs. (4) and (14). In Fig. 3, we also plot these three cases together so that one can better see the development in the tails of the appropriate q-Gaussian curve. Up to now, we have three z values that corroborate the proposed scaling relation (4): (i) $z \to 1$ gives $q = 2$ (Cauchy distribution), (ii) $z \to \infty$ leads $q = 1$

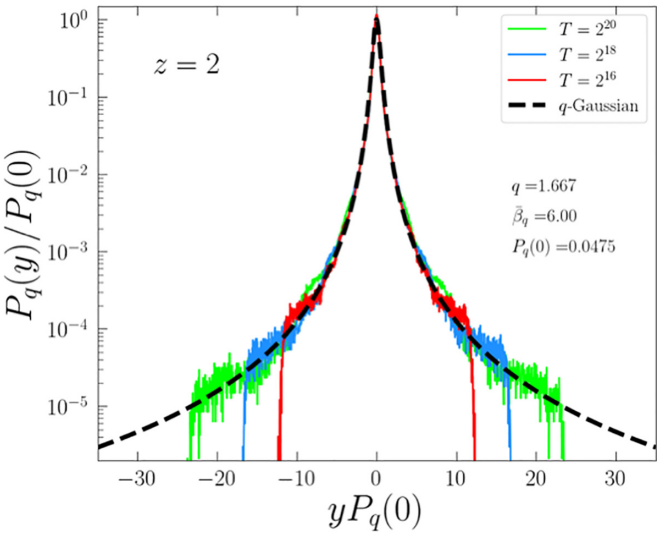

FIG. 3. Data collapse of Fig. 2. It is evident that, as (a, T) tuple simultaneously approaches $a \to a_c$ and $T \to \infty$, the simulation results become developing in the tails more and more.

(Gaussian distribution) [notice that $\lim_{z\to\infty} \lim_{|x_0|\to 1} |x_0|^z = 1$, whereas $\lim_{|x_0|\to 1} \lim_{z\to\infty} |x_0|^z = 0$, i.e., a nonuniform convergence emerges; in our parametrization, the predicted $q(z) \to 1$ reflects thinning tails (Gaussian limit)], and (iii) $z = 2$ indicates $q = 5/3$.

Now, let us numerically check four more z values (two smaller, two larger than 2) to better corroborate the scaling relation. As the z values differ from 2 along both directions, it becomes numerically harder to simulate. This is the reason why we choose z values not too distant from 2. In all obtained cases, we use the quadruple precision instead of double precision and most probably, as z values are too far away from 2, even higher precisions will be needed. For the chosen z values ($z = 1.75, 1.85, 2.15, 2.25$), the results are given in Fig. 4. For all cases, we use the $(q, \tilde{\beta}_q)$ tuples obtained from Eqs. (4) and (14), which allows us to see a strong corroboration between the expected q-Gaussian and the numerically obtained histogram. In order to better visualize this corroboration, in Fig. 5, we plot the z dependence of $\tilde{\beta}_q$, q and $P_q(0)$. For q and $\tilde{\beta}_q$, the analytical results from Eqs. (4) and (14) are depicted as dashed black lines. The simulation results are shown as green dots, while the exact results for the $z \to 1$ case are denoted by red stars. It is also evident that, as $z \to \infty$, expected values $[(\tilde{\beta}_q, q) = (\pi, 1)]$ are approached. Finally, for a tentative heuristic relation of $P_q(0)$ with respect to z, we suggest $P_q(0) = \alpha z^{-\nu}$ with $\alpha = 0.24$ and $\nu = 2.31$.

V. CONCLUSION

We examined the central limit behavior for sums of successive iterates of the one-dimensional z-logistic map at the Feigenbaum-Coullet-Tresser accumulation point, where the Lyapunov exponent vanishes (weak chaos) and strong mixing

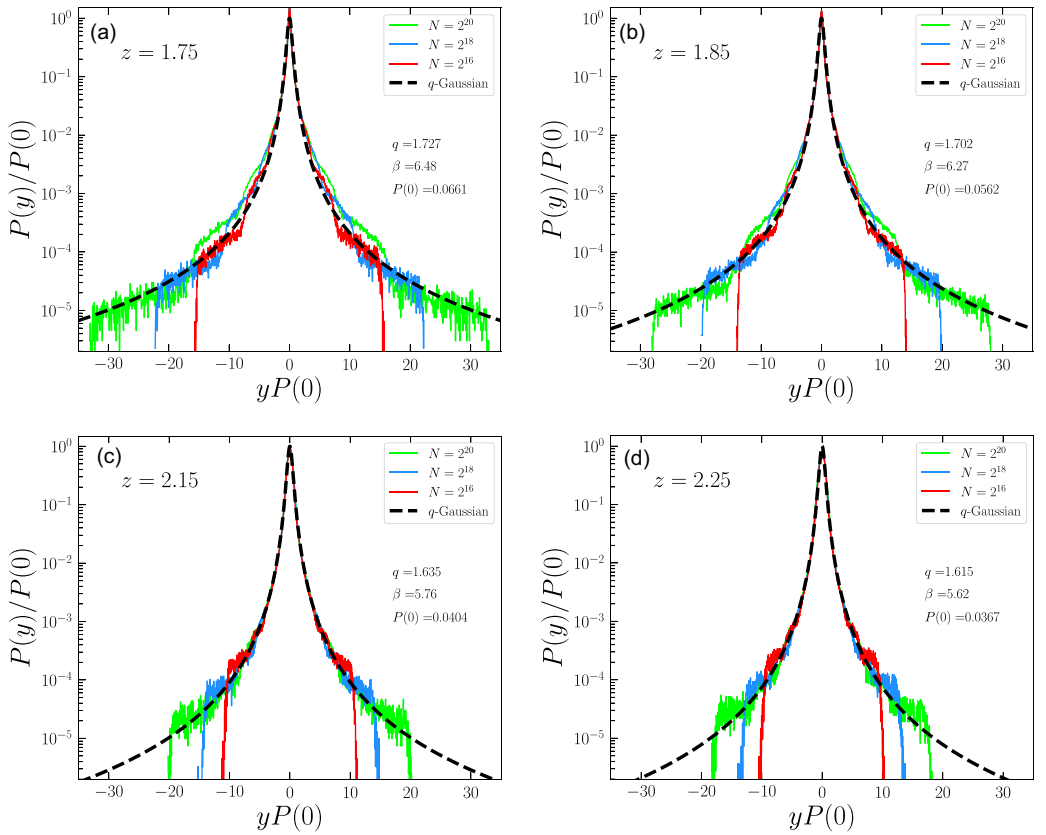

FIG. 4. Data collapse of three different (a, T) tuples for the cases $z = 1.75, 1.85, 2.15, 2.25$. The computational cost corresponding to values of z very distant from $z = 2$ exceeds our present capacities.

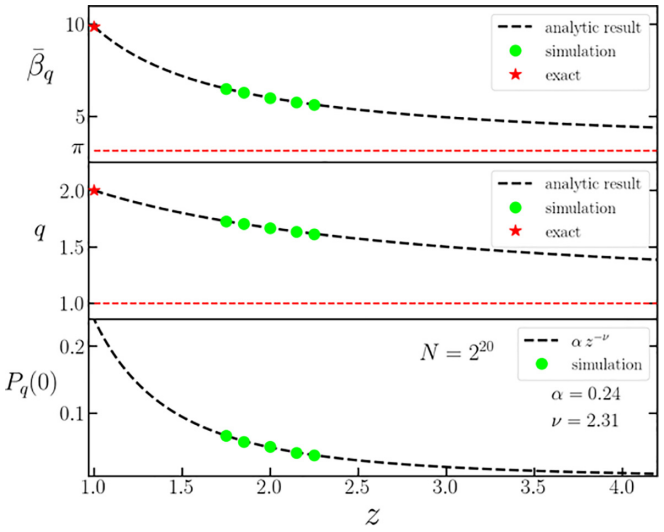

FIG. 5. Black curves are analytic and green dots are from numerics. We have that $\lim_{z\to\infty}(\bar{\beta}_q, q) = (\pi, 1)$ and $\lim_{z\to 1}(\bar{\beta}_q, q) = (\pi^2, 2)$. The tentative heuristic relation $P_q(0) = \alpha z^{-\nu}$ has been obtained from the fitting of these five green numerically obtained points. Notice that, in contrast with $P_q(0)$, q and $\bar{\beta}_q$ are not fitting parameters but are instead given by Eqs. (4) and (14), respectively.

breaks down. Guided by a tail-moment divergence criterion tied to the order z of the map maximum, we proposed a closed-form prediction for the index of the limiting law, $q(z) = 1 + 2/(z+1)$ [Eq. (4)]. Together with $\bar{\beta}_q = C_q^2$ [Eq. (14)], this fixes the q-Gaussian attractor up to an overall scale. Using Huberman-Rudnick scaling to couple the distance to criticality with the number of summands, we obtained data collapse for typical z values around 2, providing numerical support for the prediction without tuning the shape. The result organizes how the attractor evolves with z and implies a finite variance for $z > 2$ and a divergent one for $1 \leqslant z \leqslant 2$.

The $q(z)$ determined here characterizes the statistics of *sums* (the central limit attractor) and should not be confused with q_{sen} or other members of the q-triplet that quantify sensitivity or relaxation; such indices do not coincide in this setting. Our analysis consolidates and extends edge-of-chaos central limit behavior beyond the standard ($z = 2$) case to a family of unimodal maps with varying nonlinearity.

As a meaningful consequence of the present result we can mention that the relation conjectured for the solar wind observations [21,30,31], namely

$$q_{\text{sen}} = 1 - \frac{q_{\text{stat}} - 1}{2q_{\text{stat}} - 3} \tag{22}$$

does *not* apply to the present system. Indeed, for $z = 2$, we have $q \equiv q_{\text{stat}} = 5/3$ and $q_{\text{sen}} = 0.244\,487\,7\ldots$, which violate Eq. (22). In other words, the algebra governing the edge of chaos of the z-logistic maps is *not* the same that appears to govern the q-triplet associated to the solar wind [30–32].

Future work includes enlarging the z-range and precision, quantitative goodness-of-fit and model-selection tests against competing heavy-tailed laws, extension to other periodic windows, and exploring whether a renormalization-group argument can make the $m = z$ moment criterion rigorous. These directions would further clarify universality classes of weakly chaotic central limit behavior.

ACKNOWLEDGMENTS

This work was Funded by the Deutsche Forschungsgemeinschaft (DFG, German Research Foundation)—Projektnummer 557852701 (A.A.S.). The numerical calculations reported in this paper were partially performed at TUBITAK ULAKBIM, High Performance and Grid Computing Center (TRUBA resources). As a member of the Science Academy, Bilim Akademisi, Turkey, U.T. acknowledges support by the Izmir University of Economics Research Projects Fund under Grant No. BAP-2024-07. U.T. and C.T. acknowledge the Max Planck Institute for the Physics of Complex Systems in Dresden for support and hospitality during their visit. C.T. is partially supported by CNPq and Faperj (Brazilian agencies).

DATA AVAILABILITY

The data that support the findings of this article are not publicly available upon publication because it is not technically feasible and/or the cost of preparing, depositing, and hosting the data would be prohibitive within the terms of this research project. The data are available from the authors upon reasonable request.

[1] S. H. Strogatz, *Nonlinear Dynamics and Chaos* (CRC Press, London, 2024).
[2] R. C. Hilborn, *Chaos and Nonlinear Dynamics* (Oxford University Press, New York, 2000).
[3] C. Beck and F. Schlogl, *Thermodynamics of Chaotic Systems: An Introduction* (Cambridge University Press, Cambridge, UK, 1993).
[4] M. Y. Hamada, Investigating the dynamics of generalized discrete logistic map, Math. Models Methods Appl. Sci. **48**, 5325 (2025).
[5] M. Lawnik, Generalized logistic map and its application in chaos based cryptography, J. Phys.: Conf. Ser. **936**, 012017 (2017).
[6] K.-J. Moon and S. D. Choi, Reducible expansions and related sharp crossovers in Feigenbaum's renormalization field, Chaos **18**, 023104 (2008).
[7] B. Hu and J. M. Mao, Period doubling: Universality and critical-point order, Phys. Rev. A **25**, 3259 (1982).
[8] B. Hu, Introduction to real-space renormalization-group methods in critical and chaotic phenomena, Phys. Rep. **91**, 233 (1982).
[9] P. R. Hauser, C. Tsallis, and E. M. F. Curado, Criticality of the routes to chaos of the $1 - a|x|^z$ map, Phys. Rev. A **30**, 2074 (1984).
[10] J. P. Van Der Weele, H. W. Capel, and R. Kluiving, Period doubling in maps with a maximum of order z, Physica A **145**, 425 (1987).
[11] K. Briggs, A precise calculation of the Feigenbaum constant, Math. Comp. **57**, 435 (1991).
[12] V. Baladi, *Positive Transfer Operators and Decay of Correlations*, Advanced Series in Nonlinear Dynamics: Vol. 16 (World scientific, Singapore, 2000), pp. 324.

[13] U. M. S. Costa, M. L. Lyra, A. R. Plastino, and C. Tsallis, Power-law sensitivity to initial conditions within a logisticlike family of maps: Fractality and nonextensivity, Phys. Rev. E **56**, 245 (1997).

[14] U. Tirnakli, C. Beck, and C. Tsallis, Central limit behavior of deterministic dynamical systems, Phys. Rev. E **75**, 040106(R) (2007).

[15] S. Umarov, C. Tsallis, and S. Steinberg, On a q-central limit theorem consistent with nonextensive statistical mechanics, Milan J. Math. **76**, 307 (2008).

[16] S. Umarov, C. Tsallis, M. Gell-Mann, and S. Steinberg, Generalization of symmetric α-stable Lévy distributions for $q > 1$, J. Math. Phys. **51**, 033502 (2010).

[17] K. P. Nelson and S. Umarov, Nonlinear statistical coupling, Physica A **389**, 2157 (2010).

[18] M. G. Hahn, X. X. Jiang, and S. Umarov, On q-Gaussians and exchangeability, J. Phys. A **43**, 165208 (2010).

[19] S. Umarov and C. Tsallis, *Mathematical Foundations of Nonextensive Statistical Mechanics* (World Scientific, Singapore, 2022).

[20] D. Prato and C. Tsallis, Nonextensive foundation of Lévy distributions, Phys. Rev. E **60**, 2398 (1999).

[21] C. Tsallis, *Introduction to Nonextensive Statistical Mechanics–Approaching a Complex World*, 2nd ed. (Springer, 2023).

[22] C. Tsallis, Possible generalization of Boltzmann-Gibbs statistics, J. Stat. Phys. **52**, 479 (1988).

[23] O. Afsar and U. Tirnakli, Generalized Huberman-Rudnick scaling law and robustness of qq-Gaussian probability distributions, Europhys. Lett. **101**, 20003 (2013).

[24] B. A. Huberman and J. Rudnick, Scaling behavior of chaotic flows, Phys. Rev. Lett. **45**, 154 (1980).

[25] U. Tirnakli, C. Tsallis, and C. Beck, Closer look at time averages of the logistic map at the edge of Chaos, Phys. Rev. E **79**, 056209 (2009).

[26] D. Lai and G. Chen, Generating different statistical distributions by the Chaotic skew tent map, Int. J. Bifurcat. Chaos **10**, 1509 (2000).

[27] C. Beck, U. Tirnakli, and C. Tsallis, Generalization of the Gauss map: A jump into Chaos with universal features, Phys. Rev. E **110**, 064213 (2024).

[28] M. A. Pires, C. Tsallis, and E. M. F. Curado, Composing α-Gauss and logistic maps: Gradual and sudden transitions to Chaos, Phys. Rev. E **112**, 034209 (2025).

[29] A. Bountis, J. J. Veerman, and F. Vivaldi, Cauchy distributions for the integrable standard map, Phys. Lett. A **384**, 126659 (2020).

[30] L. F. Burlaga and A. F. Vinas, Multi-scale probability distributions of solar wind speed fluctuations at 1 AU described by a generalized Tsallis distributions, Geophys. Res. Lett. **31**, L16807 (2004).

[31] C. Tsallis, M. Gell-Mann, and Y. Sato, Asymptotically scale-invariant occupancy of phase space makes the entropy S_q extensive, Proc. Natl. Acad. Sci. USA **102**, 15377 (2005).

[32] J.-P. Gazeau and C. Tsallis, Moebius transforms, cycles and q-triplets in statistical mechanics, Entropy **21**, 1155 (2019).